

CASE FILE COPY

N69-38182

NASA CR. 106008

W & M 18

VERSATILE LIQUID HELIUM SCINTILLATION COUNTER OF LARGE VOLUME DESIGN*

D. C. Buckle,[†] J. R. Kane, B. D. Orrick

R. T. Siegel, R. J. Wetmore

Department of Physics, College of William and Mary

Williamsburg, Virginia, U. S. A.

NGA-47-006-008

*Supported in part by the National Aeronautics and Space Administration.

[†]National Aeronautics and Space Administration Predoctoral Trainee
1966-1968.

ABSTRACT

A 3 liter liquid helium counter has been assembled and used in two experimental configurations. The operation of the scintillation chamber is described in terms of these experiments, and the pulse height and resolution characteristics of the counter are given for the case where two 5 in. diam phototubes view the liquid helium with good geometry.

1. Introduction

We report design and performance characteristics for a multiwindowed liquid helium scintillation counter of 3 liter sensitive volume. The counter can be described as a 6 in. diam right cylinder which 1) can be terminated on both ends with demountable windows (either sapphire or beryllium), and 2) can be coupled with its main cylindrical axis oriented horizontally as tail section to a 15 liter helium cryostat.⁽¹⁾ With minor modifications this dewar has served as combination target-counter for two stopped-meson experiments: a) study of the depolarization of negative muons in He^4 ⁽²⁾, and b) the observation of μ^- and π^- K-series x-rays in He^4 ⁽³⁾.

The role of the helium counter in these experiments is presented in Section 2. Details of the counter's operation and assembly are given in Section 3. Finally in Section 4 measurements are reported of the counter's pulse height response when viewed by two 5 in. diam photomultiplier tubes through 5 in. diam sapphire windows.

2. Experimental Applications

2.1 Negative Muon Depolarization in Helium.

Figure 1 shows a simple plan view of the helium counter cryostat and associated plastic scintillation counters in the counter telescope of the μ^- depolarization experiment. For this work negative pions were extracted from the 600 MeV synchrocyclotron at the NASA Space Radiation Effects Laboratory; muons from pions decaying backward in the pion rest frame were then selected and brought to rest in the

helium chamber. A spin precession technique was used to measure the μ -e decay asymmetry; details of the method are given in Ref. 2.

The counter is shown housed within its LN^2 thermal shield and vacuum jacket and surrounded by a three-axis set of Helmholtz coils. The circular coils were operated at precession field strengths of either 100G or 1.5G, uniform to 1% and 10%, respectively, over the sensitive helium volume; the square transverse coils were used to nullify stray horizontal field components. In this experiment a stainless steel endplate was mounted into one of the window positions. Scintillation events in the helium were viewed through a 5 in. diam sapphire window by a single 2 in. diam phototube (Phillips 56 AVP). The tube was situated beyond the radius of the precession field coils, in thermal contact with the LN^2 shield. Optical coupling between the window and the phototube was provided by a 10 in. long aluminum foil light cone which was spray-coated with white paint (Tygon-SB-361) for diffuse reflectivity.⁽⁴⁾ An aluminum-foil liner (dashed lines in Fig. 1) was positioned inside the target cylinder. This was spray-coated with 25 mg/cm^2 of white Tygon paint followed by a deposition of $100 \text{ } \mu\text{g/cm}^2$ of p,p' diphenystilbene (DPS) which served to waveshift the primary ultraviolet scintillations in helium. The sapphire window was coated, as well, with $25 \text{ } \mu\text{g/cm}^2$ of DPS.

By operating the liquid target as a counter in this experiment we found that not only could the helium counter, No. 3, be used to define a stopping muon, i.e., $1234\overline{5}$, but its fast scintillation lifetime of approximately 6 nanoseconds also permitted the detection of the subsequent μ -decay electron, the signature for which was given

by $\overline{2345}$. These two coincidence signals formed the stop and start inputs, respectively, to a 50 MHz digital timer capable of analyzing 8 μ sec of the μ -e time spectrum. Requiring the observation of both events in the helium counter permitted the rejection of μ -e events originating from muons stopping in either the front or back walls.

2.2 Mesic X-Rays in Helium.

For the initial observation of μ^- and π^- x-rays in helium the meson counter telescope was modified from that shown in Fig. 1 to include a water Cerenkov counter for the rejection of electrons in the beam and a 4 in. x 4 in. plastic counter placed immediately before the target cryostat. Reference 3 describes this setup in which the helium counter consisted of a single chamber viewed by a 5 in. diam photomultiplier tube (RCA 4465). The value of the helium counter in x-ray work was tested during this run by comparing π^- in helium x-ray signal-to-noise for 1) a stopping meson coincidence which incorporated the helium scintillation pulse, and 2) one which did not use this information. Using the helium as a counter increased the x-ray signal-to-noise by a factor of two.

Figure 2 provides a detailed two-view schematic of the counter as modified for a second x-ray run. This arrangement featured on one end of the target cylinder a beryllium window unit W_1 (3 in. diam aperture by 0.040 in. thickness) which permitted the transmission of soft mesic x-rays, and on the other end an optical window unit W_2 consisting of two 2 in. diam commercial sapphire windows. (5)

A liner of aluminum foil and thin mylar construction partitioned the chamber into two separate scintillation compartments which

in our counter scheme were labeled He-4 and He-5. The details of this liner are evident from Fig. 3, while its location and orientation within the counter cryostat is specified by dashed lines in both views of Fig. 2. Of particular interest is the vertical partition of 0.0005 in. thick aluminized mylar. The interior portions of the liner received the same reflector-waveshifter coating described in Section 2.1. The liner was then assembled upon a thin aluminum frame, and inserted into the counter by removing one of the windows. A transparent layer of DPS ($25 \mu\text{g}/\text{cm}^2$) also coated the inner surface of the sapphire windows. Photomultiplier tubes PM-4 (Phillips 56 TVP) and PM-5 (Phillips 56 AVP) were cooled by a demountable copper extension to the LN^2 radiation jacket and connected to external tube bases through 20 pin feedthroughs. Cross-talk between these phototubes caused by light from one compartment window reaching the other compartment's phototube was suppressed by a copper baffle located between them. Tests in which a light pulser placed in one compartment emitted a saturation signal in that phototube showed no light leakage to the adjacent section.

A two-compartment design of this type was chosen to facilitate measurement of the absolute yield of μ^- and π^- K-series x-rays in helium. In this particular study mesons were brought to rest in counter He-4, with He-5 operated in anticoincidence. With thin mylar as the back wall to He-4 we were able to reduce considerably the number of mesons which stopped in the downstream wall and hence were able to determine more accurately the number of true stops in the liquid helium. The major portion of the running time, however, was given to the measurement of x-ray energy, linewidth, and relative transition yields.

For this latter work signals from the counters He-4 and He-5 were mixed to increase the detection rate for helium x-rays.

Helium mesic x-rays in the energy range from 8 to 14 keV were detected by an $80 \text{ mm}^2 \times 3 \text{ mm}$ thick Si(Li) detector.⁽⁶⁾ This detector was mounted in a separate LN^2 coldfinger housing and was coupled to a cooled FET (the first stage of the preamplifier) using the design of Shuler and Harris.⁽⁷⁾ Figure 2 shows an imploded design for the helium counter vacuum jacket which made it possible for the Si detector to come to within 2 in. of the helium window W_1 . A total of five walls were located between the liquid helium and the Si detector itself:

- 1) 0.0005 in. aluminized mylar as that part of the liner next to W_1 ,
- 2) beryllium window W_1 , 3) a LN^2 thermal shield of 0.0005 in. mylar,
- 4) a vacuum jacket beryllium window (1 in. diam by 0.010 in. thickness),
- and 5) a window similar to 4) on the top hat of the Si(Li) coldfinger housing. The transmission coefficient for this sequence of windows was 81% for the $\pi\text{-K}_\alpha$ energy of 10.8 keV.⁽⁸⁾

3. Assembly and Operation of the Counter

Figure 4 depicts the various indium O-ring seals made for the target chamber. The manner in which the target section was coupled to the helium reservoir section of the cryostat (neck seal) is shown in Fig. 4a. This consisted in compressing a ring of 3/32 in. diam indium wire between flanges of stainless steel.⁽⁹⁾ Compression to a thickness of 0.010 in. was achieved by drawing together a pair of split rings which made contact to the flanges. Excessive tightening of the eight screws was prevented by inserting a thin split collar of proper

height (not shown in Fig. 4a) at the outer edge of the rings. Stainless steel was the common material used in the three target seals. To reduce thermal emissivity the outer surfaces of these gasket assemblies were silver plated.

Figure 5b shows a partially-exploded view of the beryllium window seal. Two indium O-rings of 3/32 in. thickness were chosen to seal a 6 in. diam by 0.040 in. thick disk of beryllium in a recessed target flange of 6 3/4 in. i.d.⁽¹⁰⁾ The seal was made by threading a retaining cap over the flange and tightening eight screws mounted within the cap. In practice we made a permanent sandwich of the beryllium disk between its containing rings by using eight flat-head screws (not shown in the figure) to compress the smaller diameter O-ring. The aperture for x-rays could be varied by attaching to the sandwich, metal rings of selected internal diameter. If large aperture were required this design could be modified for a 5 in. diam view.

Figure 4c shows the double sapphire window plate used in the x-ray yield experiment, while Fig. 4d is a schematic of the 5 in. diam window. Both type sapphire window units were commercially supplied, each consisting of a sapphire disk brazed into a tantalum or kovar ring.⁽⁵⁾ Each window plate fit a recessed target flange, making a seal with one indium O-ring. With few exceptions these indium O-ring seals were easy to make and were tight to a helium leak detector under repeated cycling to liquid helium temperatures. The opening of a window seal required two lock-nut screws which passed through the retaining cap and threaded into positions on the window unit. Locking the nuts against the top of the retaining cap the screws were then able to withdraw the window unit from the flange.

4. Test of Pulse Height Uniformity

One of our initial aims with the helium counter was to demonstrate that a uniform pulse height response in liquid helium could be achieved with a two-window configuration. The experimental arrangement took the following form: Five inch diam sapphire windows were mounted in the counter chamber and each was viewed by an RCA 4465 photomultiplier tube (5 in. diam with S-20 response) at a window-to-photocathode separation of 1/2 in. An aluminum-foil liner conformed to the inside of the 6 in. diam chamber, and received the following preparation: 18 mg/cm² of white Tygon paint followed by a 100 µg/cm² evaporation layer of DPS waveshifter. The target faces of the sapphire windows were coated with 30-40 µg/cm² of DPS.

Po²¹⁰ was electrodeposited on a 0.001 in. diam SS wire, and the wire in turn secured to a long 1/8 in. diam SS tube which extended from the target region to the top of the cryostat, allowing manipulation of the source. A schematic insert in Fig. 5 shows the view of the counter looking down this 1/8 in. tubing. The tube is off the center-line of the cryostat by 1.5 in. along the X-axis. Within the chamber a thin wire extension to this tubing lies in the horizontal plane and is represented by the arrow in Fig. 5. To the tip of this arrow the source wire is attached in a vertical orientation. Full rotation of the 1/8 in. diam tube swung the source from the center of the counter, to the sapphire window B and back to center, with pulse height measurements being taken in steps of 45°. Vertical displacement along the Z-axis allowed us to map the Z diameter at the center of the counter and at the window.

Phototube pulses were shaped in a stretcher-amplifier and presented to a 400 channel PHA. For a given position of the alpha source anode pulses A and B were analyzed both separately and in a summed form $A + B$ using a fan-in circuit. Before taking data the signals from A and B were placed in coincidence and matched in pulse height with the source located at the center of the counter, $X = Y = Z = 0$.

The results obtained in the $Z = 0$ plane as a function of the source's X component of displacement are given in Fig. 5a. The symmetry of the counter allows us to anticipate an identical response in the negative X region. With window B located at $X = 3.25$ in., the $A + B$ response was found to be uniform to within $\pm 2\%$ over the central 80% of the X traversal. Typical $A + B$ pulse height resolution at any given source position, however, was 16% (FWHM).⁽¹¹⁾

In Fig. 5b we display the $A + B$ response vs Z displacement at fixed angles $\theta = 0, \pi/2$, and π . Included are the overlapping individual responses from phototubes A and B with the source at the center, $\theta = 0$.

Figures 4a and 4b together show that considerably more variation in $A + B$ pulse height exists across a diameter than along the X center line. It is probable that this effect could be reduced or eliminated by applying reflector-waveshifter to the exposed metal portions of the window assembly which were not so coated in this test.

We wish to acknowledge the considerable work of Mr. S. Hummel and the members of his machine shop in the development and modification of this detector cryostat, and to thank Mr. D. Makowiecki for the development of the stretcher-amplifier and tube bases. We also thank

Mr. B. Spence for his assistance during the preparation and execution of the experiments described.

FIGURE CAPTIONS

- Fig. 1 Schematic diagram of the helium counter as used in the study of the negative muon's spin depolarization in liquid helium.
- Fig. 2 Detailed schematic of the counter as modified to observe μ^- and π^- in helium x-rays. a. Downstream view. b. Plan view of the A-A cross-section.
- Fig. 3 Aluminum foil liner used to determine the absolute x-ray yields for μ^- and π^- in helium. A thin wall of mylar partitions the liquid helium into two separate counter compartments.
- Fig. 4 Various windows and gasket seals for the target chamber. a. Neck seal of target to reservoir. b. Beryllium window mounted in flange. c. Two sapphire window unit, and d. 5 in. diam sapphire window.
- Fig. 5 Pulse height response of counter in two window configuration. a. Individual (A or B) and combination (A + B) pulse height uniformity in X direction. b. Individual and combination response in Z direction.

REFERENCES

1. Sulfrian Cryogenics, Inc., Rahway, New Jersey.
2. D. C. Buckle, J. R. Kane, R. T. Siegel, and R. J. Wetmore, Phys. Rev. Letters 20, 705 (1968).
3. R. J. Wetmore, D. C. Buckle, J. R. Kane, and R. T. Siegel, Phys. Rev. Letters 19, 1003 (1967).
4. U. S. Stoneware Co., Akron, Ohio.
5. Ceramaseal, Inc., New Lebanon Center, New York.
6. Technical Measurements Corp. Detector Type 80-3AA.
These detectors are now available from Kevex Corp. Burlingame, California.
7. R. J. Harris, Jr., and W. B. Shuler, Nucl. Instr. and Methods 51, 341 (1967).
8. R. T. McGinnies, U. S. Nat. Bur. Stand Supplement to Circular 583 (1959).
9. Indium Corp. of America, Utica, New York.
10. Brush Beryllium Co., Cleveland, Ohio.
11. In the past we have achieved a resolution of 8% (FWHM) using a 1/4 liter helium chamber viewed by a single EMI 8558 photomultiplier. J. R. Kane, R. T. Siegel, and A. Suzuki, Rev. Sci. Instr. 34, 817 (1963).

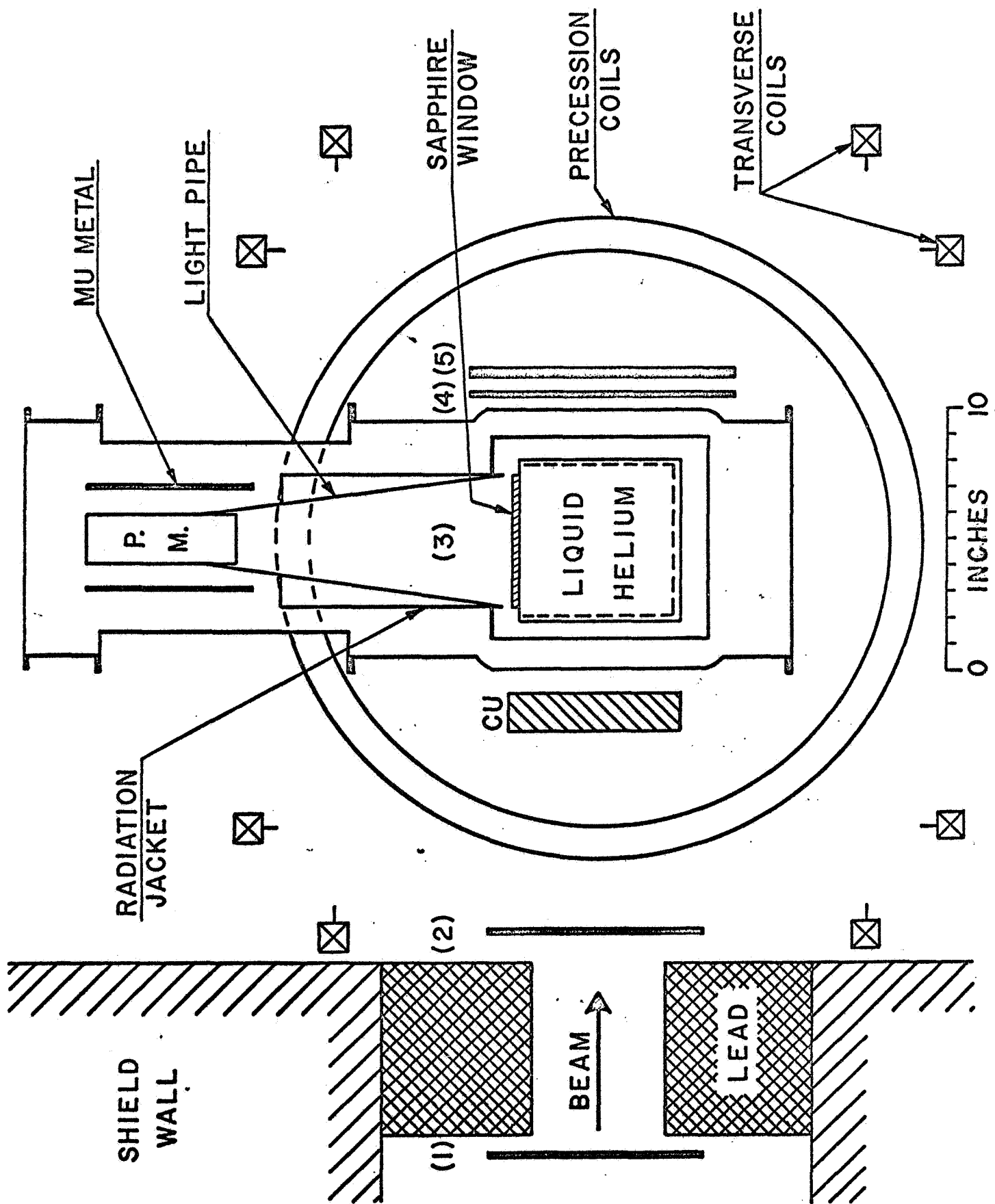


FIG. 1

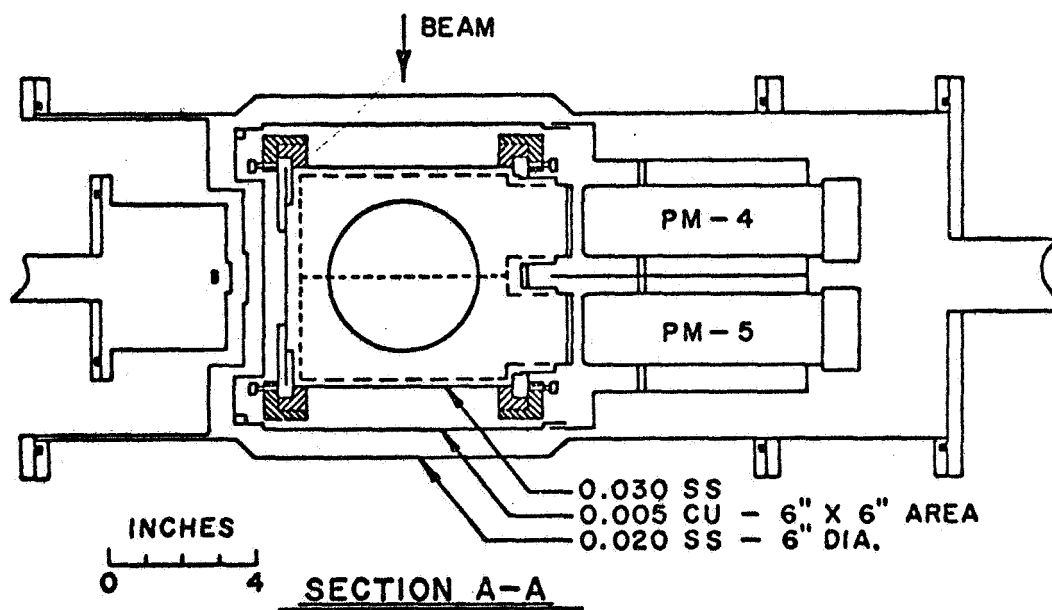
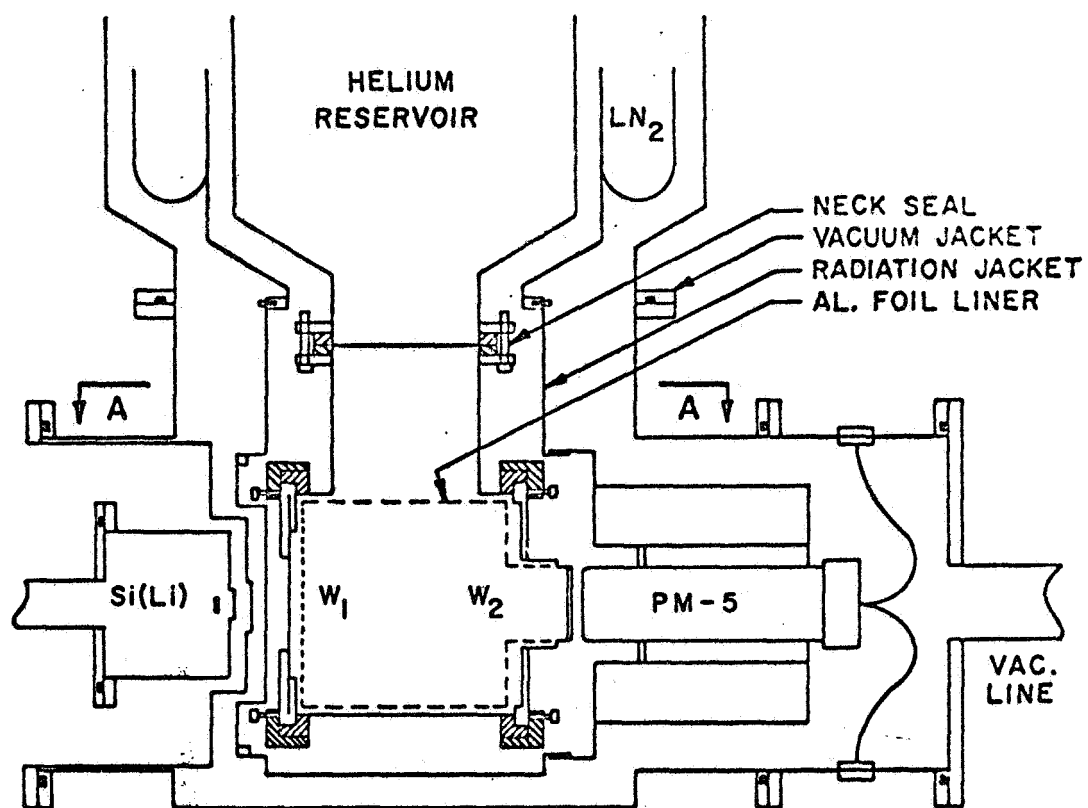


FIG. 2

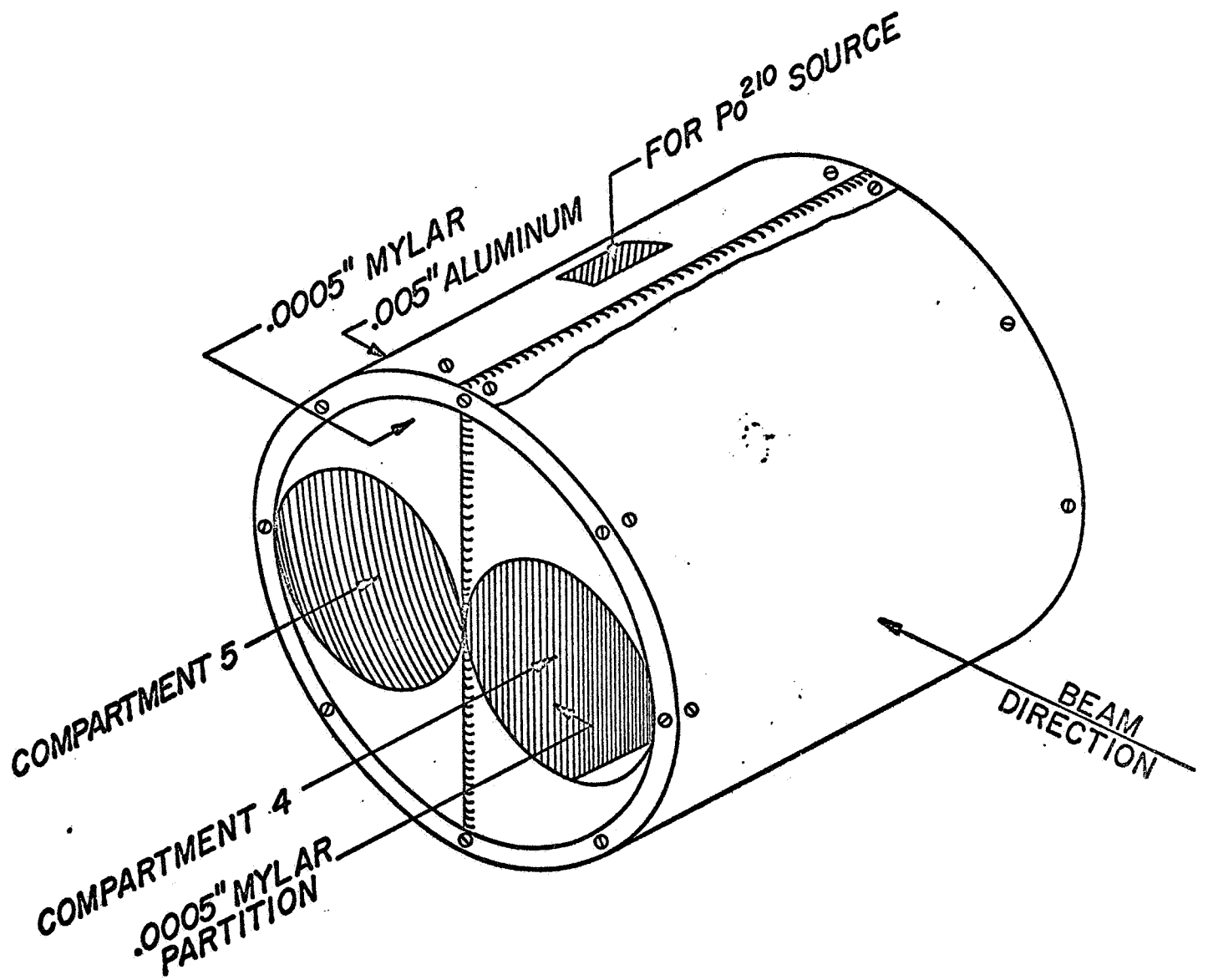


FIG. 3

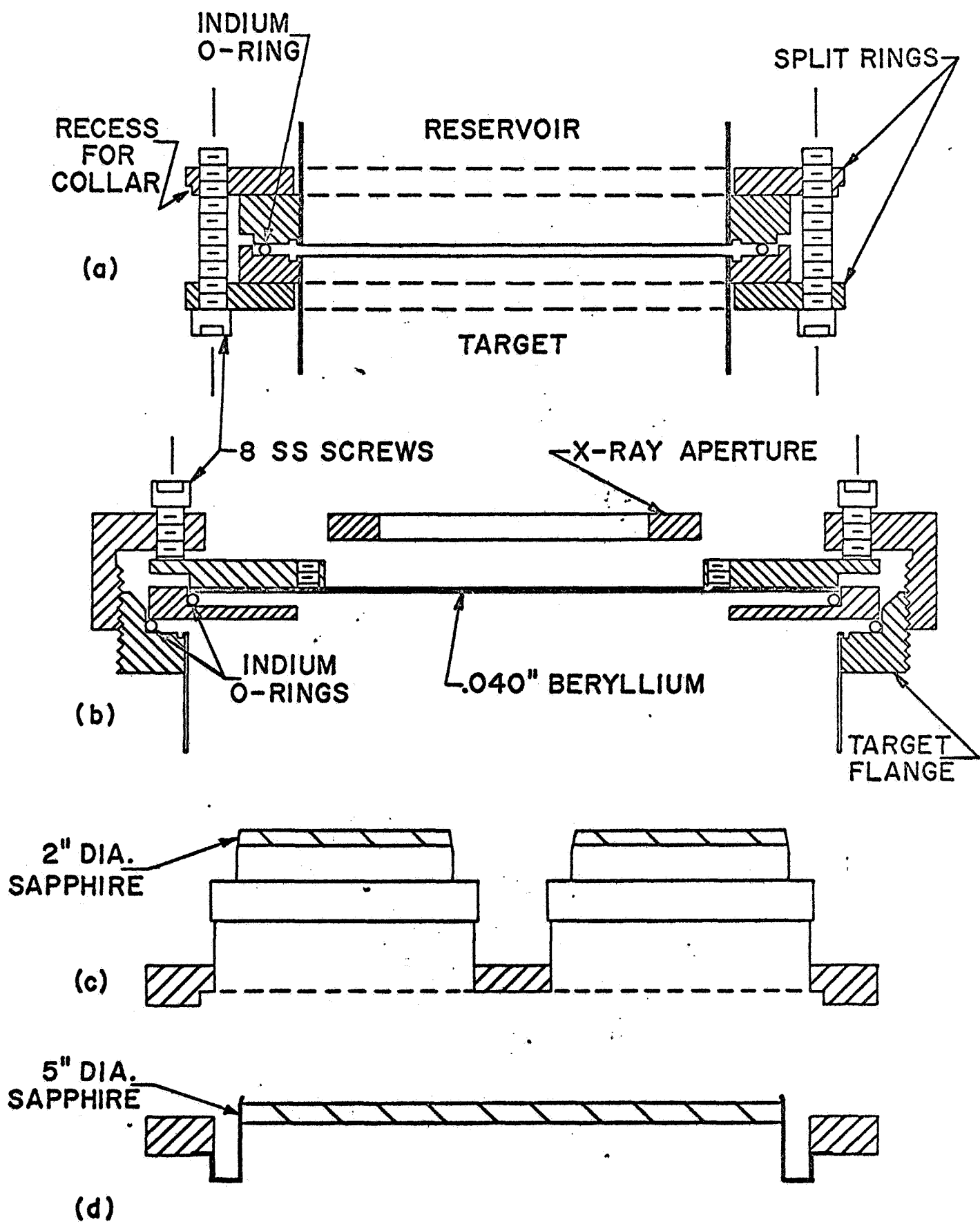


FIG. 4

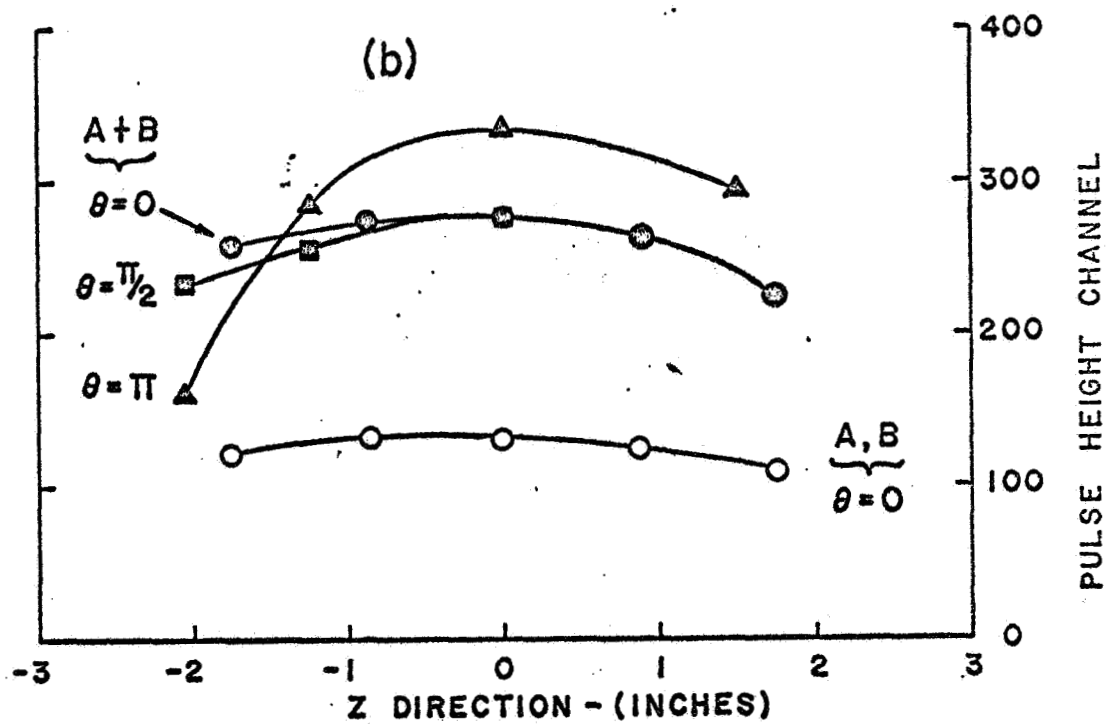
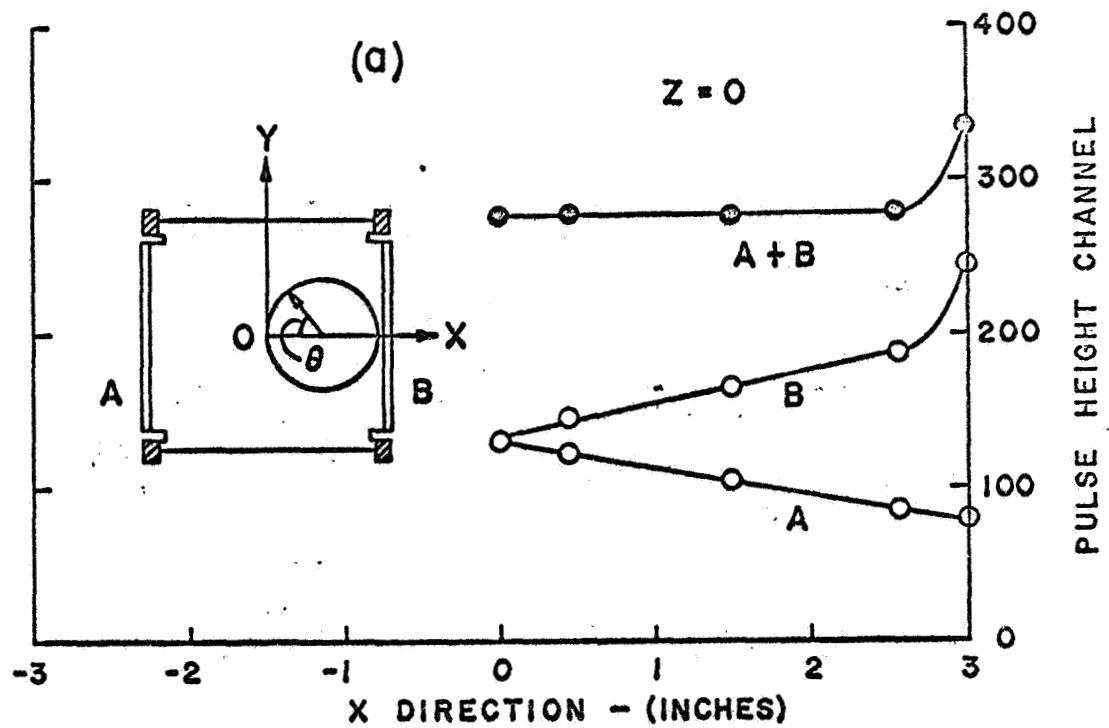


FIG. 5